

# Engineering a Small HOMO-LUMO Gap and Intramolecular B–B Hydroarylation by Diborene/Anthracene Orbital Intercalation

Sunewang R. Wang, Merle Arrowsmith, Julian Böhnke, Holger Braunschweig,\* Theresa Dellermann, Rian D. Dewhurst, Hauke Kelch, Ivo Krummenacher, James D. Mattock, Jonas H. Müssig, Torsten Thiess, Alfredo Vargas, Jiji Zhang

**Abstract:** The diborene **1** was synthesized by reduction of a mixture of 1,2-di-9-anthryl-1,2-dibromodiborane(**6**) and trimethylphosphine with potassium graphite. The X-ray structure of **1** shows the two anthryl rings to be parallel and their  $\pi(C_{14})$  systems perpendicular to the diborene  $\pi(B=B)$  system. This twisted conformation allows for intercalation of the relatively high-lying  $\pi(B=B)$  orbital and the low-lying  $\pi^*$  orbital of the anthryl moiety with no significant conjugation, resulting in a small HOMO-LUMO gap (HLG) and ultimately an unprecedented anthryl B–B bond hydroarylation. The HLG of **1** was estimated to be 1.57 eV from the onset of the long wavelength band in its UV–vis absorption spectrum (THF,  $\lambda_{\text{onset}} = 788$  nm). The oxidation of **1** with elemental selenium afforded diboraselenirane **8** in quantitative yield. By oxidative abstraction of one phosphine ligand by another equivalent of elemental selenium, the B–B and C<sup>1</sup>–H bonds of **8** were cleaved to give the cyclic 1,9-diboraanthracene **9**.

Since the first definitive synthesis of a doubly base-stabilized diborene by Robinson and coworkers in 2007,<sup>1</sup> much progress has been made in the synthesis and reactivity of this family of reactive compounds.<sup>2,3,4</sup> However, given the limits of competent Lewis bases and substituents, isolable neutral diborenes are still relatively few.<sup>2d,3m,4</sup> Thus far, only heteroaromatic rings, such as furyl, have been shown to stay coplanar with the diborene  $\pi(B=B)$  system,<sup>3c,f</sup> allowing their  $\pi$  systems to conjugate. On the other hand, we envisage that  $\pi$ -electron systems in twisted aryl-substituted diborenes<sup>3b,d,k</sup> may provide a scaffold to intercalate the low-lying  $\pi^*$  orbitals of arenes, such as anthracene and longer acenes,<sup>5</sup> into the diborene  $\pi(B=B)$  frontier orbitals to engineer a small HOMO-LUMO gap (HLG), even in the absence of  $\pi$ -conjugation (Figure 1).<sup>3g,6</sup> A torsion angle of 90° between  $\pi(B=B)$  and  $\pi(\text{aryl})$  systems would be the ideal conformation for this purpose. In our previous studies, such torsion angles in

NHC-stabilized<sup>3b</sup> and phosphine-stabilized<sup>3d,k</sup> diborenes were found to be 54° and 88°, respectively. With this in mind, DFT calculations were first carried out to elucidate the possibility of frontier orbital intercalation in anthryl-substituted diborene **1**, with the choice of phosphine ligand  $\text{PMe}_3$  rather than NHC ligands. As shown in Figure 1, the HOMO of **1** is mainly a B–B  $\pi$ -bonding orbital, while the LUMO is completely located on the anthryl moieties, which consists of in-phase LUMOs of anthracene.<sup>7</sup> The LUMO+1, consisting of anti-phase LUMOs of anthracene and a small amount of B–B  $\sigma$ -bonding character, is almost degenerate with the LUMO. Such pseudo-degeneracy is also observed for HOMO-1/-2.<sup>7</sup> These results clearly demonstrate a strong electronic decoupling in the frontier orbital intercalation of diborene and anthracene in **1**.

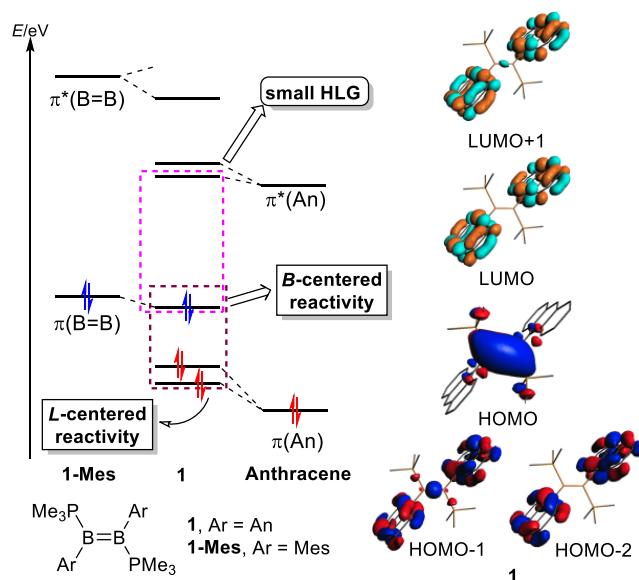


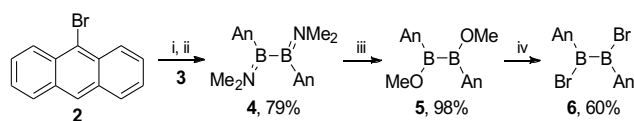
**Figure 1.** Schematic of the frontier orbital intercalation between anthracene and diborene frontier orbitals in **1**.

The extremely electron-rich B=B double bond of diborenes completely dominates their reactivity (B-centered reactivity as shown in Figure 1), usually leaving the substituents intact, which play exclusively the role of protecting groups.<sup>2d</sup> However, in the orbital intercalation case of dianthryldiborene **1**, electrons in HOMO-1/-2, originating from the highest-energy anthryl-based orbitals, may allow further transformations (L-centered reactivity as shown in Figure 1). Herein, the synthesis, characterization and reactivity of 9-anthryl-substituted diborene **1** are reported, which has a HLG as small as 1.57 eV. In the presence of an excess of elemental selenium, the B=B bond is oxidized,

- [a] Dr. S. R. Wang, Dr. M. Arrowsmith, J. Böhnke, Prof. Dr. H. Braunschweig, Dr. T. Dellermann, Dr. R. D. Dewhurst, H. Kelch, Dr. I. Krummenacher, J. H. Müssig, T. Thiess  
Institut für Anorganische Chemie  
Julius-Maximilians-Universität Würzburg  
Am Hubland, 97074 Würzburg (Germany)  
and  
Institute for Sustainable Chemistry and Catalysis with Boron  
Julius-Maximilians-Universität Würzburg  
Am Hubland, 97074 Würzburg (Germany)  
E-mail: h.braunschweig@uni-wuerzburg.de
- [b] J. D. Mattock, Dr. A. Vargas  
Department of Chemistry, School of Life Sciences, University of Sussex  
Brighton BN1 9QJ, Sussex (UK)
- [c] Dr. J. Zhang  
Department of Chemistry and Center of Novel Functional Molecules,  
The Chinese University of Hong Kong  
Shatin, New Territories, Hong Kong (China)

followed by hydroarylation and cleavage of the B–B single bond by an anthryl C<sup>1</sup>–H bond, an unprecedented reactivity pattern for diborenes.<sup>3j,l</sup>

To synthesize **1**, the new precursor 1,2-dibromodiborane(4) **6** was first prepared as orange needles from 9-bromoanthracene **2** and 1,2-dibromo-1,2-bis(dimethylamino)diborane(4) **3** in four steps in an overall yield of ca. 50% (Scheme 1).<sup>7,8</sup> Compounds **4–6** were fully characterized by <sup>1</sup>H, <sup>11</sup>B, and <sup>13</sup>C{<sup>1</sup>H} NMR spectroscopy and elemental analysis. Their structures were further confirmed by X-ray crystallography, as shown in Figure 2.<sup>7</sup> While the boron–boron bond lengths of these diboranes(4) vary little upon changing the substituents [1.713(4), 1.723(4), and 1.669(9) Å for **4–6**, respectively], the <sup>11</sup>B NMR signals are significantly shifted downfield from 52.1 ppm (**4**) and 64.0 ppm (**5**) to 92.5 ppm (**6**).<sup>8</sup>



**Scheme 1.** Preparation of 1,2-dibromodiborane(4) **6**. Reagents and conditions: (i) BuLi (1.05 equiv), Et<sub>2</sub>O, –30 °C to rt, 2 h; (ii) **3** (0.5 equiv), Et<sub>2</sub>O, –78 °C to rt, then reflux, 3 h; (iii) HCl (4.2 equiv), MeOH (25 equiv), Et<sub>2</sub>O, –78 °C, 2 h, then rt, 20 h; (iv) BBr<sub>3</sub> (2.5 equiv), CH<sub>2</sub>Cl<sub>2</sub>, –30 °C to –10 °C, 1 h. An = 9-anthryl.

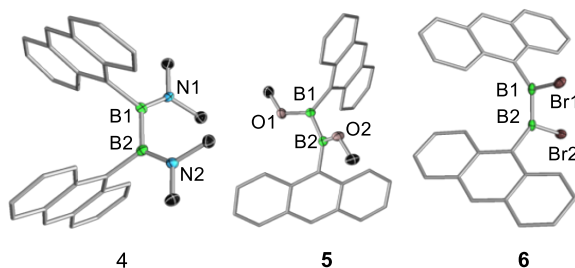
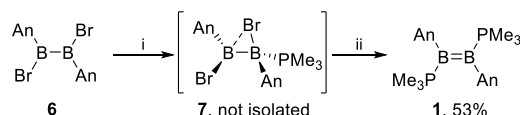


**Figure 2.** Molecular structures of **4**, **5**, and **6**. Thermal ellipsoids are shown at the 50% probability level. Hydrogen atoms are omitted for clarity.

The one-pot synthesis of diborene **1** was achieved by reduction of the phosphine adduct of **6** with excess potassium graphite (KC<sub>8</sub>) in the presence of PMe<sub>3</sub> in benzene (Scheme 2).<sup>3d,k,7</sup> The intermediate adduct **7** was not isolated,<sup>9</sup> as the yellow precipitate in the first step was not stable enough in solution to allow NMR spectroscopic characterization. This suggests that the anthryl group may lead to further reactivity (see below). Following recrystallization from the green-blue benzene solution, diborene **1** was obtained as dark-green air-sensitive crystals in 53% yield. The diborene moiety in **1** was readily identified by its characteristic <sup>11</sup>B NMR signal at  $\delta$  = 22.0 ppm and broad <sup>31</sup>P{<sup>1</sup>H} NMR signal at  $\delta$  = –21.3 ppm, comparable with that of the mesityl analogue **1-Mes** ( $\delta_B$  = 16.7 and  $\delta_P$  = –24.4 ppm, respectively).<sup>3k</sup> The boron–boron distance of **1** was found to be 1.524(6) Å (Figure 3).<sup>7,10</sup> This is relatively short in comparison to reported B=B double bonds (1.55–1.63 Å), yet substantially longer than B≡B triple bonds (around 1.45 Å).<sup>2d,3a</sup> The anthryl rings were found to be mutually parallel, and their  $\pi$ (C<sub>14</sub>) systems are perpendicular to that of the diborene  $\pi$ (B=B) system.



**Scheme 2.** Synthesis of diborene **1**. Reagents and conditions: (i) PMe<sub>3</sub> (2.5 equiv), benzene, rt, 0.5 h; (ii) KC<sub>8</sub> (5.0 equiv), benzene, rt, 5 h. An = 9-anthryl.

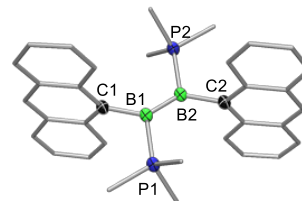


**Figure 3.** Molecular structure of **1**. Thermal ellipsoids are shown at the 50% probability level. Hydrogen atoms are omitted for clarity. Selected bond lengths [Å] and angles [°]: B1-B2 1.524(6), B1-C1 1.620(6), B1-P1 1.903(5), B2-B1-C1 133.5(3), B2-B1-P1 116.6(3), C1-B1-P1 109.7(3).

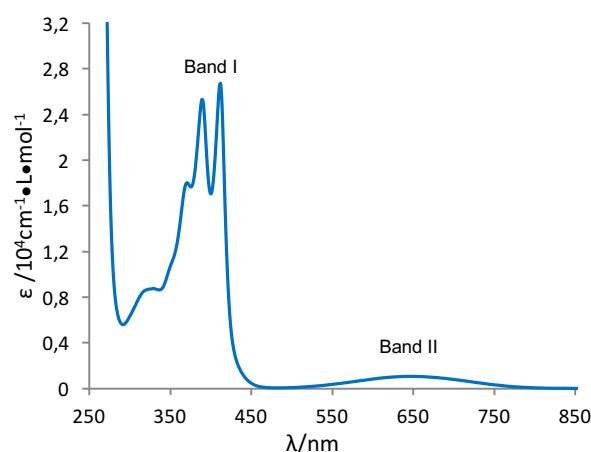
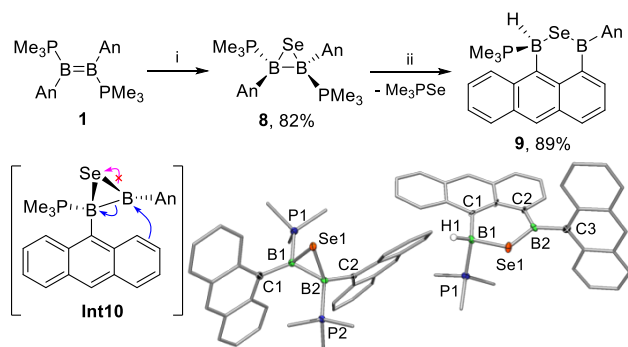


**Figure 4.** UV-vis absorption spectrum of **1** in THF.

The solution UV-vis absorption spectrum of the dark-green diborene **1** in THF showed an intense structured band at 300–460 nm (band I,  $\epsilon$  26.8 × 10<sup>3</sup>) and a weak but distinct absorption band at 645 nm (band II,  $\epsilon$  1094) (Figure 4). The fine structure of band I, with local maxima at  $\lambda$  = 376, 390 nm,  $\lambda_{\text{max}}$  at 412 nm and a shoulder at  $\lambda$  = 321 nm, can be attributed to the <sup>1</sup>L<sub>a</sub> band of the anthryl moieties overlapped with the band from the B=B double bond, as dilute solutions of anthracene and its derivatives are well-known to show structured absorption spectra at around 330–380 nm,<sup>11</sup> while reported phosphine-stabilized trans-diborenes show broad absorptions at around 330–450 nm.<sup>3d,k</sup> Due to the compound's limited solubility and stability, the solvent polarity effect on band II could not be extensively studied,<sup>12</sup> although it shows the characteristics of intramolecular charge-transfer (ICT) absorption bands.<sup>13</sup> These spectral features are in good accord with the picture that the  $\pi$ (B=B) and  $\pi$ (C<sub>14</sub>) systems are independent of each other and that there is no significant conjugation between the two  $\pi$  systems in solution, as expected from the mutually perpendicular arrangement of the two  $\pi$  systems observed in the crystal.

Cyclic voltammetry in THF revealed a single reversible oxidation event for **1** at  $E_{\text{ox}} = -0.89$  V vs. ferrocene/ferrocenium. This is slightly more positive than that of the reported phosphine-stabilized *trans*-diborenes (around  $-1.05$  V), suggesting that the diborene is a slightly weaker reductant.<sup>3d,k</sup> Although the HOMO of **1** is subtly stabilized by interaction with the anthryl groups in comparison to that of **1-Mes** (Figure 1), a small HLG was achieved by intercalation of the anthryl-located orbitals between the orbitals related to the B=B double bond – usually the frontier orbitals of diborenes (Figure 1). As commonly reported for small-HLG molecules, the onset of the long-wavelength UV-vis absorption in THF was determined to be  $\lambda_{\text{onset}} = 788$  nm,<sup>7</sup> which corresponds to a band gap of 1.57 eV. This value is markedly smaller than HLG values calculated for other phosphine-stabilized diborenes (3.5–5.8 eV),<sup>3d,k</sup> and even NHC-stabilized analogues, which have significantly smaller HLGs (2.1–2.7 eV).<sup>3d,m</sup>

The oxidation of **1** with elemental selenium was then conducted to validate the reactivity of the anthryl-substituted diborene (Scheme 3).<sup>7</sup> Similar to the recently reported reactions of NHC-stabilized diborenes and diborynes,<sup>3j,l</sup> diborene **1** reacted readily with one equivalent of  $\text{Se}^0$  to quantitatively afford the desired diboraselenirane **8** as monitored by  $^1\text{H}$  NMR spectroscopy. Compound **8** was isolated in 82% yield by recrystallization from benzene/hexane. An  $^{11}\text{B}$  NMR signal of **8** in  $\text{C}_6\text{D}_6$  was found at  $-17.8$  ppm, in accord with that of a doubly NHC-bound diboraselenirane.<sup>3l</sup> The molecular structure of **8** was further confirmed by X-ray crystallography (Scheme 3). Interestingly, further exposure of **8** to elemental selenium resulted in a slow but clean transformation to a new compound (**9**) over two days, with emergence of  $^{11}\text{B}$  NMR signals at  $-17.9$  and  $79.1$  ppm. Along with this change in the  $^{11}\text{B}$  NMR spectrum,  $^1\text{H}$  NMR signals from the anthryl hydrogens split into nine sets with a total integral of 17 hydrogens, indicating the occurrence of the anthryl C–H bond functionalization. In the  $^{31}\text{P}\{^1\text{H}\}$  NMR of the reaction mixture, the emergence of a sharp signal at 5.85 ppm with characteristic  $^{77}\text{Se}$  satellites ( $^1J_{\text{P-Se}} = 713$  Hz) clearly indicated the formation of  $\text{Me}_3\text{PSe}$ .<sup>14</sup> An X-ray diffraction analysis of suitable single crystals of **9** determined the molecular structure to be the 1,9-diboraanthracene derivative shown in Scheme 3. Furthermore, a doublet signal at 4.84 ppm for one hydrogen ( $^2J_{\text{P-H}} = 11.6$  Hz) was observed in the  $^1\text{H}\{^{11}\text{B}\}$  NMR spectrum of **9** by setting the decoupler offset to  $-18$  ppm, confirming the presence of the BH moiety in **9**.<sup>7</sup>



**Scheme 3.** Reactions of diborene **1** with elemental selenium, and crystallographically-determined structures of reaction products **8** (left) and **9** (right). Reagents and conditions: (i)  $\text{Se}^0$  (1.3 equiv),  $\text{C}_6\text{D}_6$ , rt, sonication, 5 min; (ii)  $\text{Se}^0$  (excess),  $\text{C}_6\text{D}_6$ , rt, 2 d. An = 9-anthryl. Thermal ellipsoids are shown at the 50% probability level. Hydrogen atoms (except for that on B1 atom of **9**) and solvent molecules (benzene in **9**) are omitted for clarity. Selected bond lengths [Å] and angles [°]. Compound **8**: B1–B2 1.749(3), B1–Se1 2.063(2), B2–

Se1 2.073(2), B1–P1 1.925(2), B2–P2 1.935(2), B1–C1 1.629(3), B2–C2 1.632(3), B2–B1–Se1 65.3(1), B1–B2–Se1 64.7(1), B1–Se1–B2 50.03(9). Compound **9**: B1–Se1 2.059(6), B2–Se1 1.900(7), B1–P1 1.941(8), B1–C1 1.610(9), B2–C2 1.56(1), B2–C3 1.60(1), B1–Se1–B2 100.0(3), Se1–B1–P1 103.6(3), Se1–B1–C1 116.8(4), Se1–B2–C3 123.1(5), Se1–B2–C3 115.7(5), C2–B2–C3 121.1(6).

Compound **9** may result from the cleavage of the B–B bond of diboraselenirane **8** by the anthryl  $\text{C}^1\text{–H}$  bond, initiated by oxidative abstraction of one  $\text{PMe}_3$  ligand followed by the nucleophilic attack from the anthryl  $\pi$ -electrons to the electron-deficient tricoordinate boron in **Int10** (Scheme 3).<sup>15,16</sup> In the ring-opening reaction of the proposed intermediate **Int10**, the cleavage of the Se–B bond is unexpectedly disfavored over that of the B–B bond, despite the fact that formation of a selenide as a leaving group is easier than that of a boryl anion or radical. This reveals the unique reactivity of diboraseleniranes, since seleniranes are typically utilized as intermediates for the synthesis of alkenes in organic synthesis.<sup>17</sup>

In conclusion, the dark-green 9-anthryl-substituted diborene **1** was isolated by reduction of 1,2-di-9-anthryl-1,2-dibromodiborane(4) with  $\text{KC}_8$  in the presence of  $\text{PMe}_3$ . The X-ray structure of **1** shows the two anthryl rings to be mutually parallel, and their  $\pi(\text{C}_{14})$  systems are perpendicular to the diborene  $\pi(\text{B}=\text{B})$  system. This electronic decoupling leads to an intercalation of the frontier orbitals of the constituent B=B and anthracene systems, leading to a remarkably small HOMO-LUMO gap in the molecule. A distinct ICT absorption band at long wavelengths was detected in the UV-vis spectrum of **1**, leading to a dark green color unknown for doubly-phosphine-stabilized diborenes. Furthermore, in the presence of excess selenium, the anthryl  $\text{C}^1\text{–H}$  bond was also found to hydroarylate and cleave the resulting B–B single bond, an unprecedented reactivity pattern showing sequential reactivity of the frontier orbitals of the intercalated constituent B=B and anthracene systems. Currently, a systematic investigation of this diborene scaffold, including synthesis, photophysics, and reactivity, is underway in our group.

## Experimental Section

General experimental details, characterization data for all reported compounds and details of the DFT calculations are all included in the Supporting Information. Crystallographic data have been deposited with the Cambridge Crystallographic Data Centre as supplementary publication nos. 1542099 (**1**), 1542102 (**4**), 1542100 (**5**), 1542101 (**6**), 1542103 (**8**), 1542104 (**9**) and can be obtained free of charge via [www.ccdc.cam.ac.uk/data\\_request/cif](http://www.ccdc.cam.ac.uk/data_request/cif).

## Acknowledgements

This project was funded by the European Research Council (ERC) under the European Union Horizon 2020 Research and Innovation Program (grant agreement no. 669054). We thank the Alexander von Humboldt Foundation for postdoctoral research fellowships to S.R.W. and M.A.. A.V. thanks the University of Sussex for financial support.

**Keywords:** boron • small HOMO-LUMO gap • diborenes • borylation • hydroarylation

- [1] a) Y. Wang, B. Quillian, P. Wei, C. S. Wannere, Y. Xie, R. B. King, H. F. Schaefer, P. v. R. Schleyer, G. H. Robinson, *J. Am. Chem. Soc.* **2007**, *129*, 12412–12413. b) Y. Wang, B. Quillian, P. Wei, Y. Xie, C. S. Wannere, R. B. King, H. F. Schaefer, P. v. R. Schleyer, G. H. Robinson, *J. Am. Chem. Soc.* **2008**, *130*, 3298–3299.
- [2] a) Y. Wang, G. H. Robinson, *Chem. Commun.* **2009**, 5201–5213. b) H. Braunschweig, R. D. Dewhurst, *Angew. Chem., Int. Ed.* **2013**, *52*, 3574–3583. c) H. Braunschweig, R. D. Dewhurst, *Organometallics* **2014**, *33*, 6271–6277. d) M. Arrowsmith, H. Braunschweig, T. E. Stennett, *Angew. Chem., Int. Ed.* **2017**, *56*, 96–115.
- [3] a) H. Braunschweig, R. D. Dewhurst, K. Hammond, J. Mies, K. Radacki, A. Vargas, *Science* **2012**, *336*, 1420–1422. b) P. Bissinger, H. Braunschweig, A. Damme, T. Kupfer, A. Vargas, *Angew. Chem., Int. Ed.* **2012**, *51*, 9931–9934. c) H. Braunschweig, R. D. Dewhurst, C. Hörl, A. K. Phukan, F. Pinzner, S. Ullrich, *Angew. Chem., Int. Ed.* **2014**, *53*, 3241–3244. d) P. Bissinger, H. Braunschweig, A. Damme, T. Kupfer, I. Krummenacher, A. Vargas, *Angew. Chem., Int. Ed.* **2014**, *53*, 5689–5693. e) J. Böhnke, H. Braunschweig, W. C. Ewing, C. Hörl, T. Kramer, I. Krummenacher, J. Mies, A. Vargas, *Angew. Chem., Int. Ed.* **2014**, *53*, 9082–9085. f) H. Braunschweig, C. Hörl, *Chem. Commun.* **2014**, *50*, 10983–10985. g) P. Bissinger, H. Braunschweig, A. Damme, C. Hörl, T. Kupfer, *Angew. Chem., Int. Ed.* **2015**, *54*, 359–362. h) P. Bissinger, A. Steffen, A. Vargas, R. D. Dewhurst, A. Damme, H. Braunschweig, *Angew. Chem., Int. Ed.* **2015**, *54*, 4362–4366. i) J. Böhnke, H. Braunschweig, T. Dellermann, W. C. Ewing, T. Kramer, I. Krummenacher, A. Vargas, *Angew. Chem., Int. Ed.* **2015**, *54*, 4469–4473. j) H. Braunschweig, T. Dellermann, W. C. Ewing, T. Kramer, C. Schneider, S. Ullrich, *Angew. Chem., Int. Ed.* **2015**, *54*, 10271–10275. k) P. Bissinger, H. Braunschweig, M. A. Celik, C. Claes, R. D. Dewhurst, S. Endres, H. Kelch, T. Kramer, I. Krummenacher, C. Schneider, *Chem. Commun.* **2015**, *51*, 15917–15920. l) H. Braunschweig, T. Dellermann, W. C. Ewing, M. Hess, A. Rempel, C. Schneider, S. Ullrich, *Angew. Chem., Int. Ed.* **2016**, *55*, 5606–5609. m) H. Braunschweig, I. Krummenacher, C. Lichtenberg, J. D. Mattock, M. Schäfer, U. Schmidt, C. Schneider, T. Steffenhagen, S. Ullrich, A. Vargas, *Angew. Chem., Int. Ed.* **2017**, *56*, 889–892.
- [4] An unsymmetrical diborene has also been reported recently, see: W. Lu, Y. Li, R. Ganguly, R. Kinjo, *J. Am. Chem. Soc.* **2017**, *139*, 5047–5050.
- [5] a) R. Dabestani, I. N. Ivanov, *Photochem. Photobiol.* **1999**, *70*, 10–34. b) M. Yoshizawa, J. K. Klosterman, *Chem. Soc. Rev.* **2014**, *43*, 1885–1898.
- [6] D. F. Perepichka, M. R. Bryce, *Angew. Chem., Int. Ed.* **2005**, *44*, 5370–5373.
- [7] Experimental, spectroscopic, crystallographic, and computational details are given in the Supporting Information.
- [8] a) A. Moezzi, M. M. Olmstead, P. P. Power, *J. Chem. Soc., Dalton Trans.* **1992**, 2429–2434. b) H. Hommer, H. Nöth, J. Knizek, W. Ponikvar, H. Schwenk-Kircher, H. *Eur. J. Inorg. Chem.* **1998**, 1519–1527.
- [9] H. Braunschweig, A. Damme, J. O. C. Jimenez-Halla, T. Kupfer, K. Radacki, *Angew. Chem., Int. Ed.* **2012**, *51*, 6267–6271.
- [10] The molecule displays an inversion center and is entirely disordered in a 64:36 ratio via a mirror plane crossing the center of the B–B bond at a ca. 38° angle. The bond lengths being discussed belong to the major orientation, which was shown in Figure 3.
- [11] J. B. Birks, *Photophysics of Aromatic Hydrocarbons*; Wiley-Interscience, London, **1970**.
- [12] The UV–vis absorption spectra of **1** in THF, benzene, and fluorobenzene were obtained. Absorption maxima and extinction coefficients for band II are as follows: 645 nm ( $\epsilon$  1094), 649 nm ( $\epsilon$  1015), and 653 nm ( $\epsilon$  918). Full UV-vis spectra are included in the Supporting Information.
- [13] An ICT interaction between the silicon-based  $\pi$  systems in disilenes and silenes and 9-anthryl  $\pi$ -electron systems has been observed. See: a) T. Iwamoto, M. Kobayashi, K. Uchiyama, S. Sasaki, S. Nagendran, H. Isobe, M. Kira, *J. Am. Chem. Soc.* **2009**, *131*, 3156–3157. b) T. Iwamoto, N. Ohnishi, N. Akasaka, K. Ohno, S. Ishida, *J. Am. Chem. Soc.* **2013**, *135*, 10606–10609.
- [14] R. García-Rodríguez, H. Liu, *J. Phys. Chem. A* **2014**, *118*, 7314–7319.
- [15] For a recent review on reactivities of diboranes(4): E. C. Neeve, S. J. Geier, I. A. I. Mkhalid, S. A. Westcott, T. D. Marder, *Chem. Rev.* **2016**, *116*, 9091–9161.
- [16] An example of cleavage of the B–B bond in diborane(4) by hydrogen has been reported, see: N. Tsukahara, H. Asakawa, K.-H. Lee, Z. Lin, M. Yamashita, *J. Am. Chem. Soc.* **2017**, *139*, 2593–2596.
- [17] M. Saito, J. Nakayama, *Science of Synthesis* **2007**, *39*, 1023–1032.